

AD-A191 390

THEORETICAL CALCULATIONS OF XEF GROUND STATE KINETICS

1/1

(U) AEROSPACE CORP EL SEGUNDO CA AEROPHYSICS LAB

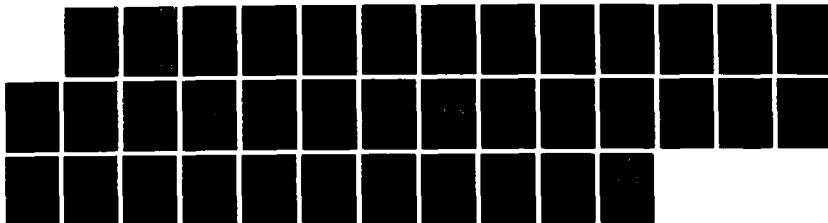
R L WILKINS 01 MAR 80 TR-0006A(2061)-1 SD-TR-8039

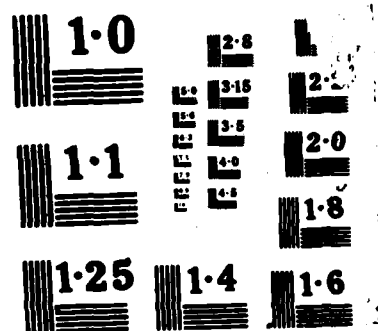
UNCLASSIFIED

F04701-85-C-0006

F/G 7/2

NL





AD-A191 398

APPROVED FOR PUBLIC RELEASE;
DISTRIBUTION UNLIMITED

DTIC
ELECTE
S *ca* D
H

88 4 4 113

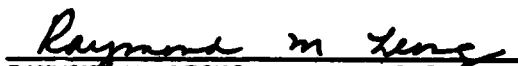
This report was submitted by The Aerospace Corporation, El Segundo, CA 90245, under Contract No. F04701-85-C-0086-P00016 with the Space Division, P.O. Box 92960, Worldway Postal Center, Los Angeles, CA 90009-2960. It was reviewed and approved for The Aerospace Corporation by W. P. Thompson, Director, Aerophysics Laboratory. Lt Scott W. Levinson/CNWD was the project officer.

This report has been reviewed by the Public Affairs Office (PAS) and is releasable to the National Technical Information Service (NTIS). At NTIS, it will be available to the general public, including foreign nationals.

This technical report has been reviewed and is approved for publication. Publication of this report does not constitute Air Force approval of the report's findings or conclusions. It is published only for the exchange and stimulation of ideas.



SCOTT W. LEVINSON, Lt, USAF
Project Officer
SD/CNWD



RAYMOND M. LEONG, Major, USAF
Deputy Director, AFSTC West Coast
Office
AFSTC/WCO OL-AB

UNCLASSIFIED

SECURITY CLASSIFICATION OF THIS PAGE

REPORT DOCUMENTATION PAGE

1a. REPORT SECURITY CLASSIFICATION Unclassified			1b. RESTRICTIVE MARKINGS		
2a. SECURITY CLASSIFICATION AUTHORITY			3. DISTRIBUTION/AVAILABILITY OF REPORT Approved for public release; distribution unlimited.		
2b. DECLASSIFICATION/DOWNGRADING SCHEDULE					
4. PERFORMING ORGANIZATION REPORT NUMBER(S) TR-0086A(2061)-1			5. MONITORING ORGANIZATION REPORT NUMBER(S) SD-TR-88-39		
6a. NAME OF PERFORMING ORGANIZATION The Aerospace Corporation Laboratory Operations		6b. OFFICE SYMBOL (If applicable)	7a. NAME OF MONITORING ORGANIZATION Space Division		
6c. ADDRESS (City, State, and ZIP Code) El Segundo, CA 90245			7b. ADDRESS (City, State, and ZIP Code) Los Angeles, CA 90009-2960		
8a. NAME OF FUNDING/SPONSORING ORGANIZATION Air Force Weapons Laboratory		8b. OFFICE SYMBOL (If applicable)	9. PROCUREMENT INSTRUMENT IDENTIFICATION NUMBER F04701-85-C-0086-P00016		
8c. ADDRESS (City, State, and ZIP Code) Kirtland Air Force Base, NM 87117			10. SOURCE OF FUNDING NUMBERS		
			PROGRAM ELEMENT NO.	PROJECT NO.	TASK NO.
					WORK UNIT ACCESSION NO.
11. TITLE (Include Security Classification) Theoretical Calculations of XeF Ground State Kinetics					
12. PERSONAL AUTHOR(S) Wilkins, Roger L.					
13a. TYPE OF REPORT		13b. TIME COVERED FROM TO		14. DATE OF REPORT (Year, Month, Day) 1988 March 1	
				15. PAGE COUNT 32	
16. SUPPLEMENTARY NOTATION					
17. COSATI CODES			18. SUBJECT TERMS (Continue on reverse if necessary and identify by block number)		
FIELD	GROUP	SUB-GROUP	Dissociation, Rotational Relaxation)		
			Excimer Lasers, Vibrational Relaxation,		
			Rate Coefficients, XeF Kinetics, XeF ₂ , Fluorine compound		
19. ABSTRACT (Continue on reverse if necessary and identify by block number)					
<p>State-to-state rate coefficients were calculated for collision-induced vibrational-to-translational (V-T) and rotational-to translational (R-T) relaxation, and for dissociation processes that occur when XeF(v,J) molecules collide with He atoms. Three-dimensional classical trajectories of the collision dynamics of these processes were calculated by means of a pairwise additive potential energy surface, which consists of a Morse function for the XeF interaction and Lennard-Jones functions for the HeXe and HeF interactions. On the basis of trajectory calculations, it is predicted that V-T relaxation and R-T relaxation occur by multi-quanta transitions, and that dissociation occurs from all the v-levels by the formation of XeF molecules in unstable rotational levels above the centrifugal barrier. As the XeF(v) molecules are carried to higher v-levels by the V-T relaxation processes, they are more easily dissociated. Both the temperature and v-dependences of the state-to-state rate coefficients were calculated for V-T and R-T relaxation and collision-induced dissociation. The V-T relaxation and dissociation processes of the XeF ground electronic state are critical in modeling XeF excimer lasers to determine their efficiency and energy extraction capabilities.</p>					
20. DISTRIBUTION/AVAILABILITY OF ABSTRACT <input type="checkbox"/> UNCLASSIFIED/UNLIMITED <input checked="" type="checkbox"/> SAME AS RPT. <input type="checkbox"/> DTIC USERS			21. ABSTRACT SECURITY CLASSIFICATION Unclassified		
22a. NAME OF RESPONSIBLE INDIVIDUAL			22b. TELEPHONE (Include Area Code)		22c. OFFICE SYMBOL

PREFACE

The author gratefully acknowledges K. L. Foster for her invaluable assistance with the calculations and the continuing interest of Dr. L. Wilson, Excimer Laser Branch, Air Force Weapons Laboratory, in this work.



Accession For	
NTIS GRA&I	<input checked="checked" type="checkbox"/>
DTIC TAB	<input type="checkbox"/>
Unannounced	<input type="checkbox"/>
Justification	
By	
Distribution/	
Availability Codes	
Avail and/or	
Dist	Special
A-1	

CONTENTS

I.	INTRODUCTION.....	9
II.	COMPUTATIONAL PROCEDURE.....	11
III.	DISCUSSION AND RESULTS.....	17
	A. Collision Dynamics.....	17
	B. State-Specific Rate Coefficients.....	24
IV.	SUMMARY.....	35
	REFERENCES	37

FIGURES

1.	Energy Level Diagram of Ground State $\text{XeF}(v, N'', e)$	12
2.	Potential Energy-Surface for Collisions of XeF Molecules with He Atoms.....	15
3.	Typical Collision-Induced Dissociation of $\text{He} + \text{XeF}(v = 6,$ $J = 10) \rightarrow \text{He} + \text{Xe} + \text{F}$	18
4.	Bond Plot for Collision-Induced Dissociation of $\text{He} + \text{XeF}(v = 6, J = 10) \rightarrow \text{He} + \text{Xe} + \text{F}$	19
5.	Force Plot of Collision-Induced Dissociation of $\text{He} + \text{XeF}(v = 6, J = 10) \rightarrow \text{He} + \text{Xe} + \text{F}$	20
6.	Typical Inelastic Collision of $\text{He} + \text{XeF}(v = 3,$ $J = 30) \rightarrow \text{He} + \text{XeF}(v' = 3, J' = 50)$	22
7.	Typical Inelastic Collision of $\text{He} + \text{XeF}(v = 0,$ $J = 10) \rightarrow \text{He} + \text{XeF}(v' = 1, J' = 13)$	23
8.	State-to-State Rate Coefficients for Collisions of XeF with He, $T = 300$ K.....	25
9.	Temperature Dependent V-T Rate Coefficients for Single Quantum Transitions for $\text{He} + \text{XeF}(v)$ Collisions.....	27
10.	Temperature Dependent Rate Coefficients for Dissociation from a Specific v-Level in $\text{He} + \text{XeF}(v)$ Collisions.....	31
11.	The v-Dependence of Rotational Relaxation of $\text{XeF}(v, J = 20)$ in Collision with He.....	32
12.	Temperature Dependence of Rotational Relaxation for Collisions of $\text{XeF}(v = 3, J = 20)$ with He.....	33

TABLES

1.	Potential Parameters.....	14
2.	State-to-State Rate Coefficients for VT Relaxation of He + XeF (v) from a Specific v-Level.....	28
3.	Rate Coefficients for Dissociation of XeF (v) in Collision with He from a Specific v-Level.....	29

1. INTRODUCTION

The XeF ground electronic state is a bound state (about 1175 cm^{-1}) of about 10 closely spaced, highly anharmonic vibrational levels.¹⁻³ The XeF ground state is not a very stable molecule because its shallow potential energy well allows rapid dissociation by collision processes. An XeF laser operates on bound-bound transitions (B-X) terminating on specific vibrational levels ($v'' = 4, 3,$ and 2) of the ground electronic state. The efficiency of an XeF laser is limited by the rate at which XeF collisions with a buffer gas remove XeF molecules from ($v'' = 4, 3,$ and 2) levels. Populations can be removed from these levels through collision-induced vibration-to-translation (V-T), collision-induced dissociation, and rotational equilibration, which carries XeF molecules to unstable rotational levels above the centrifugal barrier. A buildup of the population in this ground electronic state will destroy the population inversion of the XeF laser and thereby will terminate lasing. The efficiency and extraction capabilities are determined thus from the XeF ground state energy exchange processes and collision-induced dissociation that occur among the vibrational levels.

The V-T relaxation and dissociation of the XeF ground state have been studied at room temperature by Fulghum et al.⁴⁻⁶ using two different experimental techniques. In one experimental technique,⁴ they used a tunable pulsed ultraviolet (UV) dye laser and timing system to probe the XeF(X-B) absorption on selected vibronic transitions formed in a laser discharge. In the second experimental technique,^{5,6} they measured the XeF(B-X) emission that followed the XeF(X-B) absorption of a dye laser pulse in XeF produced by photolysis of XeF₂. Both techniques gave about the same quenching rate $(1.4 \pm 0.3) \times 10^4\text{ sec}^{-1}\text{ Torr}^{-1}$ for $v = 0$ and $v = 1$ in He and for $v = 1$ in Ne. In a similar discharge study, Gower et al.⁷ measured about the same decay rate in He as Fulghum et al.⁴⁻⁶

The experiments provide total decay rates or quenching rates and not the state-to-state rate coefficients required in kinetic modeling of XeF laser performance. Fulghum et al.⁶ developed two models to extract state-to-state V-T and dissociation rates from their experimental data. They used the

information theoretic approach of P. ocaccia and Levine⁸ to express the V-T rate coefficients. Only two parameters need to be determined by the experiments to resolve all of the V-T state-to-state rate coefficients. The overall dissociation of XeF is determined from these V-T rate coefficients and by the direct dissociation rate coefficients out of each vibrational level. The dissociation rate out of a specific vibrational level is calculated by a slight modification of the Arrhenius equation. The Arrhenius equation is multiplied by a vibrational bias parameter, which allows for a dependence of the dissociation rate on the specific level of vibrational excitation. Fulghum et al.⁶ describe the procedure for determining the two parameters required in calculating the dissociation rate coefficient from a specific vibrational level. Kiefer et al.⁹ provide a discussion of a choice for this vibrational bias parameter and some evidence that large dissociation rates are only compatible with dissociation from low vibrational states. They suggest that the dissociation from low vibrational states is assisted by rotational excitation. Neither the v-dependence nor the temperature dependence of these key rate coefficients has been measured directly. Theoretical models^{10,11} have been developed for modeling or predicting XeF kinetics. These models suffer from a lack of sufficient information for determining the many parameters of the models. State-to-state rate coefficients for vibrational and rotational, and dissociation processes of the ground state XeF in collision with inert buffer gases are required for modeling the XeF excimer laser.

The purpose of this research is to study both the temperature and v-dependences of the coupled vibrational relaxation and thermal dissociation of XeF ground electronic state in the presence of helium. Three-dimensional quasiclassical trajectory calculations have been employed to acquire both vibrational quantum number and temperature dependences of the collision-induced V-T and rotational-to-translational R-T relaxation, and to obtain dissociation rate coefficients for specific vibrational levels of ground state XeF molecules in collisions with helium atoms.

II. COMPUTATIONAL PROCEDURE

The quasiclassical Monte Carlo trajectory method has been described in a previous paper,¹² and only a brief description is provided herein. The vibrational and rotational energy levels of ^{131}XeF are calculated from the spectroscopic data given by Tellinghuisen et al.,³ which include the higher order anharmonic terms in the power series expansion in v and N'' . N'' is the angular momentum of the nuclear motion, and the quantum number N'' can have all integral values from zero up. The reactant XeF molecule is assigned vibrational quantum v and rotational quantum N'' states. Calculations are carried out for nine vibrational states, $v = 0$ through $v = 8$, and for rotational states $N'' = 0, 10, 20, 30$, and 40 . A vibration-rotation energy level diagram for ^{131}XeF is shown in Fig. 1. The spin-splitting parameters for the X state provided by Tellinghuisen et al.³ for $v = 0$ through $v = 6$ are extended to $v = 9$ by fitting a third degree polynomial to their data. The rotational energy levels are calculated for the two spin components for each N'' value. The two spin components for each N'' are labeled e or f. The label e refers to the components with $J = N'' + 1/2$, and f refers to the components with $J = N'' - 1/2$. Since the rotational energy separation between the two spin components for a given N'' is only a few wave numbers, the rotational states for the e spin component only are provided in Fig. 1. From this diagram, it is clear that some of the initial N'' values for this computation lie above the dissociation limit of XeF . In those cases, the initial N'' values employed were: for $v = 6$, $N'' = 0, 10, 20$, and 30 ; for $v = 7$, $N'' = 0, 10$, and 20 ; and for $v = 8$, $N'' = 0, 10$, and 20 . A minimum of 400 trajectories are calculated for each (v, N'') state of XeF at seven collision energies starting from 0.5 through 6.5 kcal/mole in intervals of 1.0 kcal/mole. The value of the maximum impact parameter, b_{max} , at a given energy represents the smallest value of the impact parameter for which 100 randomly chosen trajectories give neither vibrational nor rotational energy transfer nor induced dissociation. The value of the maximum impact parameter is taken to be $11.7 a_0$. A value of $18.0 a_0$ is assumed for the initial relative separation of the He atom and the center of mass of the XeF molecule. The actual technique for calculating the partitioning of the internal energy of the product species has been described

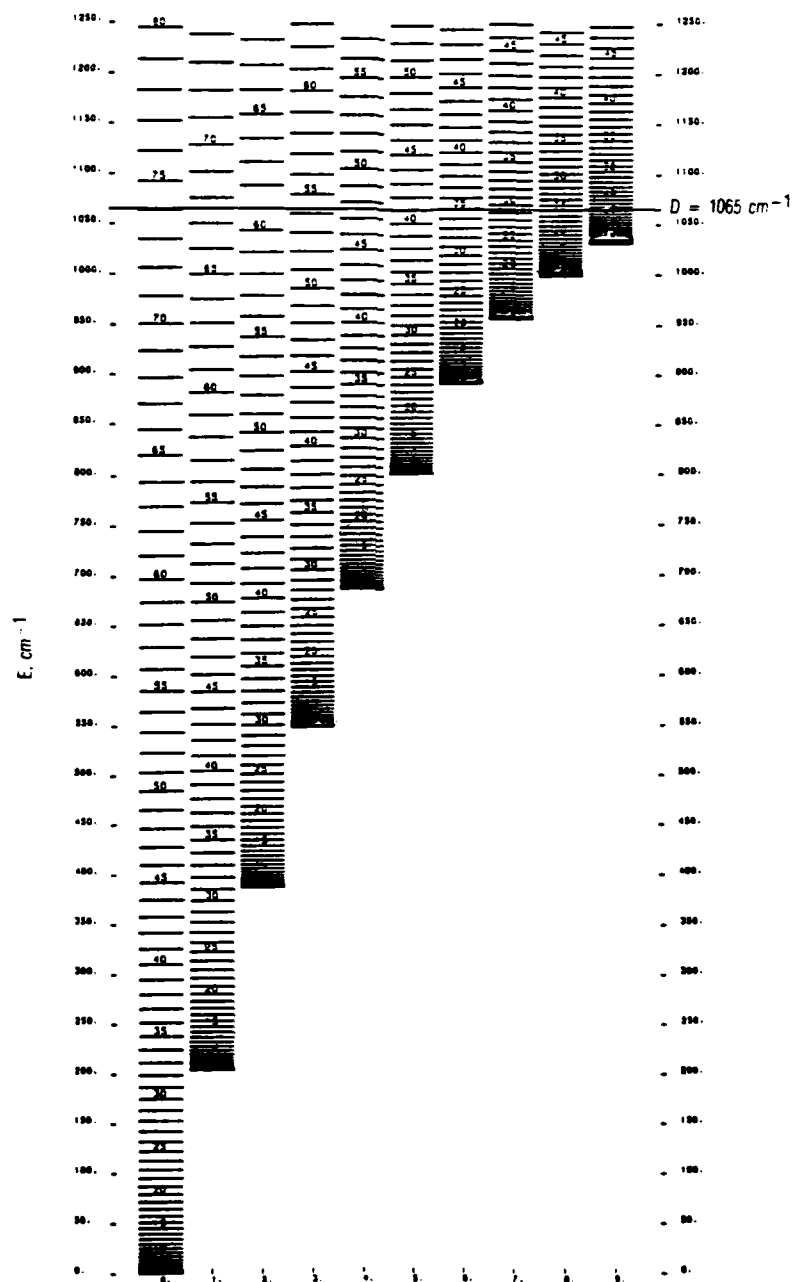


Fig. 1. Energy Level Diagram of Ground State $\text{XeF}(v, N, e)$. The letter e refers to the spin component with $J = N + 1/2$; D_0 is bond energy measured from the $v = 0$ level to the dissociation limit of XeF and has a value of 1065 cm^{-1} .

adequately¹³ and will not be repeated here. The trajectory product pair is counted as dissociated if its internal energy exceeds the height of the rotational barrier or if the internuclear separation of the product pair exceeds $7.0 a_0$.

Before modeling the collision dynamics, a reasonable potential energy surface must be constructed. The potential employed here for the He-XeF interaction is constructed by summing pairwise functions, a Morse function for the XeF interaction, and a Lennard-Jones function for the HeXe and the HeF interactions. The values of the Morse potential parameters for XeF are taken from Tellinghuisen et al.³ The values of the Lennard-Jones parameters for HeF interactions are taken from Thompson,¹⁴ and those for HeXe interactions are calculated using the theoretical data provided by Svehla.¹⁵ The potential parameters for the Morse potential and the Lennard-Jones potentials are listed in Table 1. These parameters for the Lennard-Jones potentials produce the potential curve for HeXe interaction that compares favorably with one reported by Schneider¹⁶ in his study of potential curves of xenon with other rare gas atoms. Schneider used the model for the forces between closed shell atoms developed by Gordon and Kim¹⁷ to investigate the ground state potential energy curves of Xe-Xe, Xe-He, Xe-Ne, Xe-Ar, and Xe-Kr. He found agreement between the experimentally determined values of the distance between the nuclei at the potential minimum and the depth of the potential well. The agreement was very good considering the simplicity of the calculations.

The constructed potential energy surface for He-XeF interaction is shown in Fig. 2. The parameters used to construct this potential surface are not chosen by matching any experimental data on XeF kinetics. The repulsive part of this potential is the most critical feature that affects the vibrational relaxation and dissociation.

Table 1. Potential Parameters.

Morse Function (XeF) ³		
$D_e = 3.35 \text{ kcal/mol}$		
$\alpha_e = 1.726 \text{ a.u.}^{-1}$		
$r_e = 4.367 \text{ a.u.}$		
Lennard Jones Function ^{14, 15}		
Pair	$\epsilon(\text{ev})$	$\sigma(\text{a.u.})$
HeF	0.001747	5.076
HeXe	0.003964	6.335

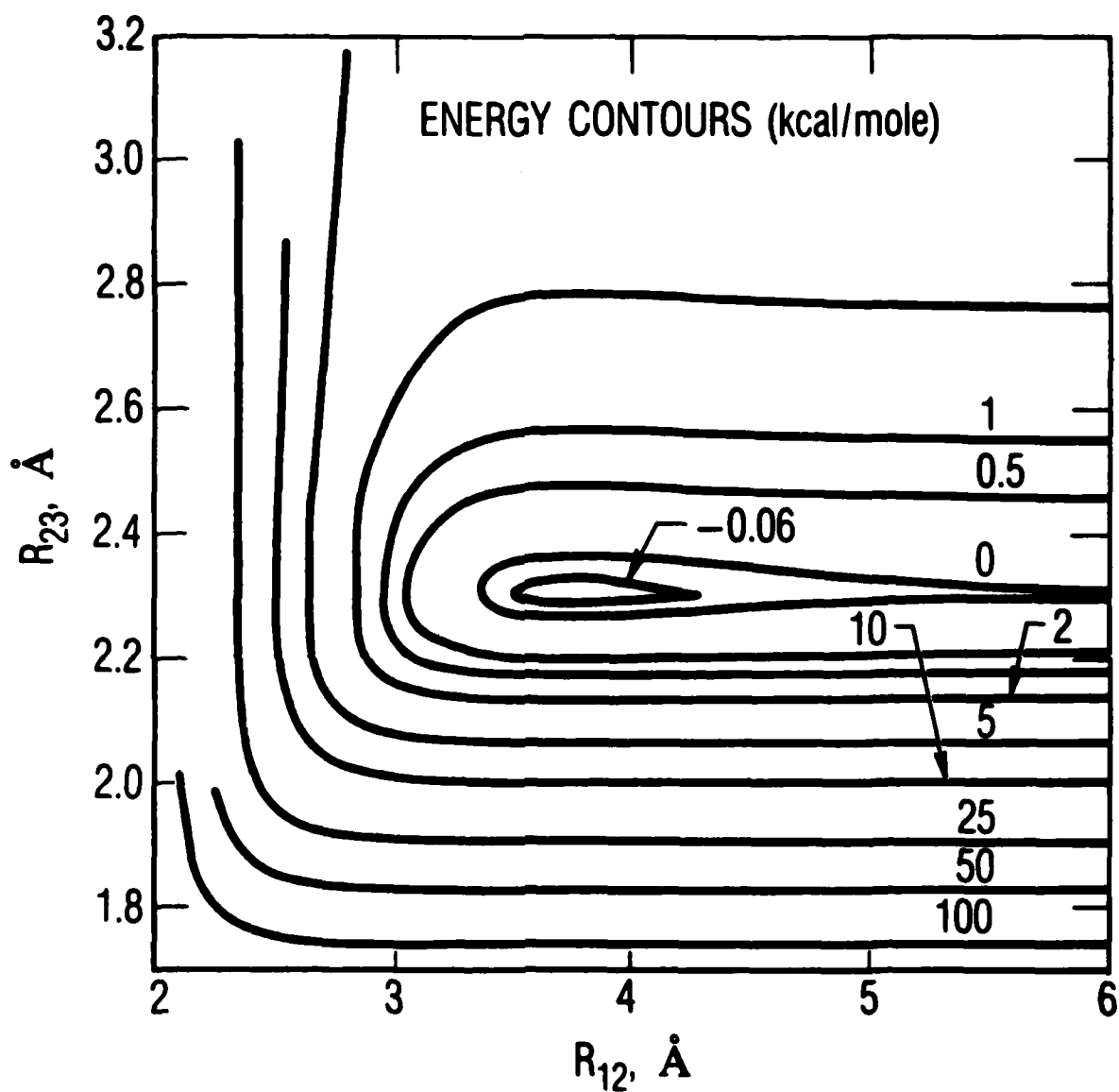


Fig. 2. Potential Energy-Surface for Collisions of XeF Molecules with He Atoms. R_{23} is the internuclear distance between the Xe and F atoms; R_{12} is the internuclear distance between the He and Xe atoms. The energy contours are in units of kcal/mole, and the R_{ij} distances are in units of \AA .

III. DISCUSSION AND RESULTS

A. COLLISION DYNAMICS

A typical collision-induced dissociation reaction between He atoms and XeF molecules is shown in Fig. 3. When the XeF bond is extended during the Xe-F vibration, the He and the Xe atoms start to attract from a considerable separation. The oscillatory trajectory moves toward smaller R_{12} values, and thus the He atom is pulled closer to the Xe atom. Finally, the representative mass point reaches a point on the surface where repulsion sets in between the He and the Xe atoms and between the Xe and F atoms. At this point, sufficient initial relative translational energy is converted into vibrational energy to dissociate the XeF molecule. The major energy transfer process is the conversion of relative translational energy into vibrational energy, T-V, and the minor energy transfer process is the conversion of rotation energy into vibrational energy, R-V. The XeF molecule can be dissociated directly from any v-level by this T-V energy transfer process. This study shows that an XeF molecule in any v-level with $J = 0$ can dissociate directly without climbing a vibrational ladder involving a sequence of single quantum energy transfer steps followed by dissociation from the topmost v-level. The bond and force plots for this same trajectory are shown in Figs. 4 and 5, respectively. The bond plot shows that direct interaction occurs and that the lifetime of the transition state is short compared to the oscillatory frequency of XeF($v = 6$, $J = 10$). The force plot shows the forces operating between the three atoms. The operative forces during an encounter have three components: F_{12} , F_{23} , and F_{13} . These three force components are shown in Fig. 5 as a function of time. A positive value of the force component corresponds to a repulsive force, a negative value to an attractive force. The forces between the end atoms are low throughout and are indicated by the dotted and dashed curves. The F_{23} component indicates that at the switch-over point, $t/T_0 = 3$, sufficient translational energy has been converted into vibrational energy of the vibrationally excited XeF molecule to dissociate the XeF molecule. This is shown as a solid line in Fig. 5, and it shows that repulsion sets in once the switch-over point is reached.

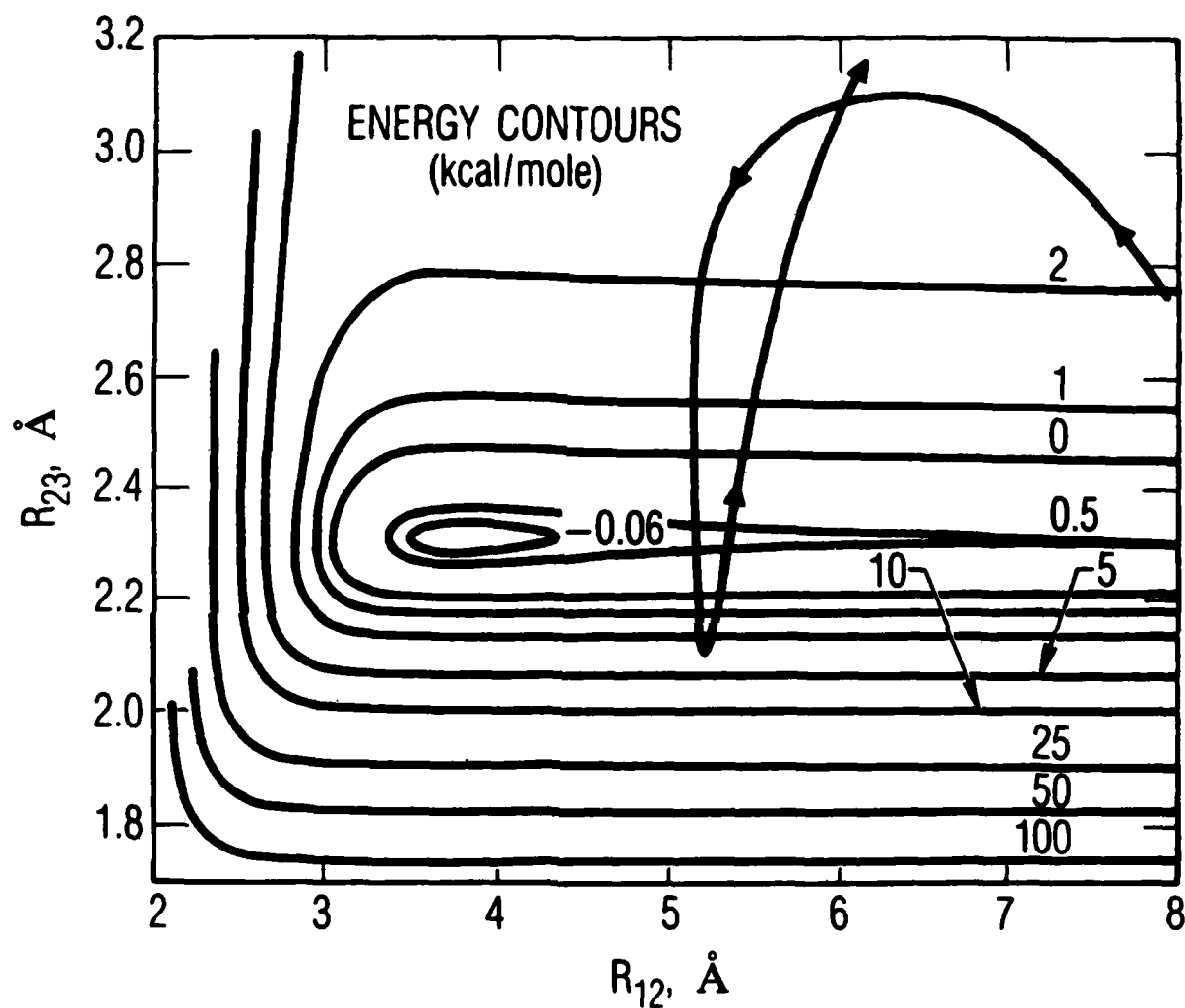


Fig. 3. Typical Collision-Induced Dissociation of $\text{He} + \text{XeF}(v = 6, J = 10) \rightarrow \text{He} + \text{Xe} + \text{F}$. The values of initial $E_{\text{TRANS}} = 1.5$ kcal/mole. For this system, T-V energy transfer is the major energy transfer process, and R-V energy transfer is the minor energy transfer process.

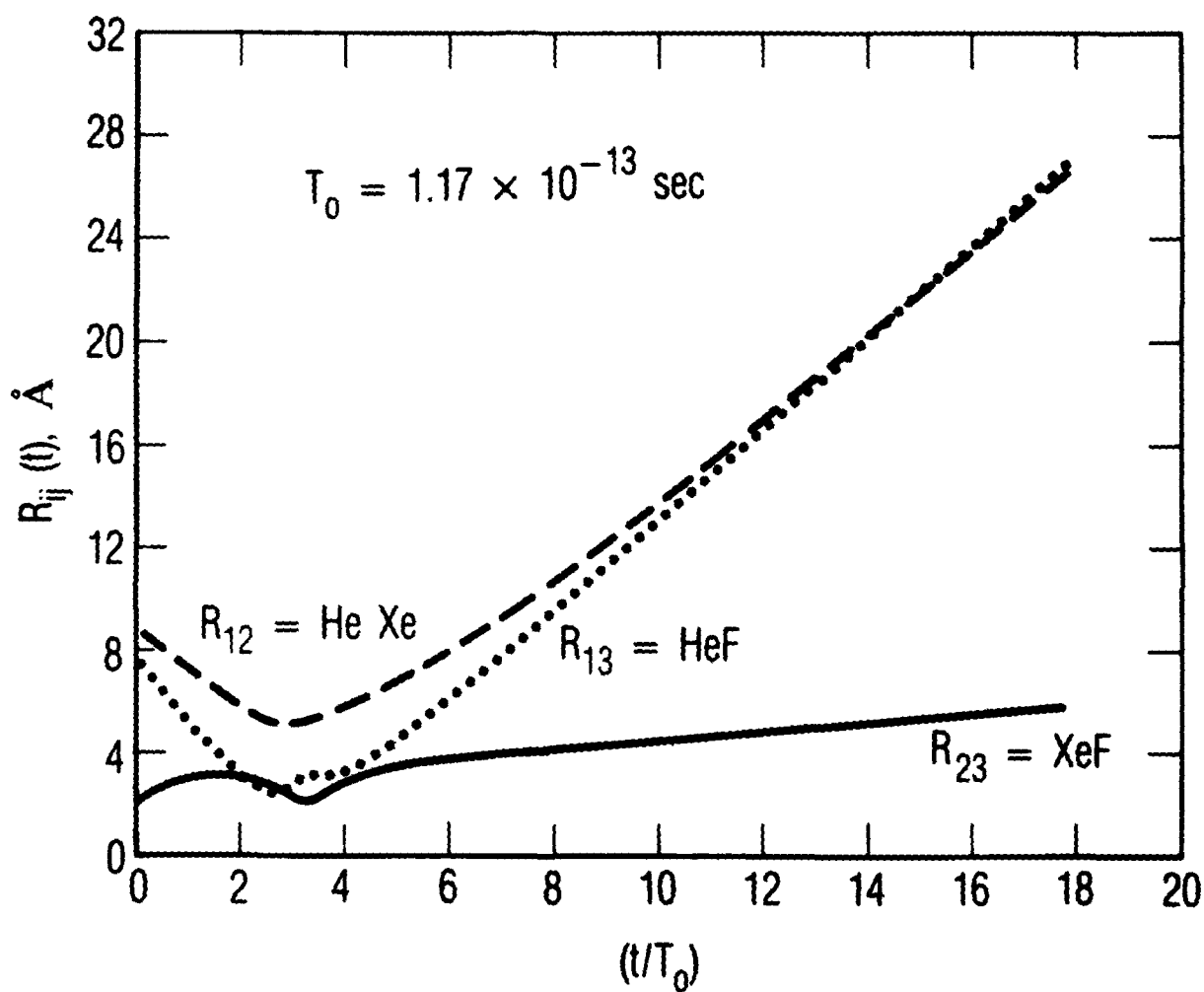


Fig. 4. Bond Plot for Collision-Induced Dissociation of $\text{He} + \text{XeF}(v = 6, J=10) \rightarrow \text{He} + \text{Xe} + \text{F}$. $T_0 = 1.17 \times 10^{-13} \text{ sec}$. This reaction occurs by a direct interaction mechanism.

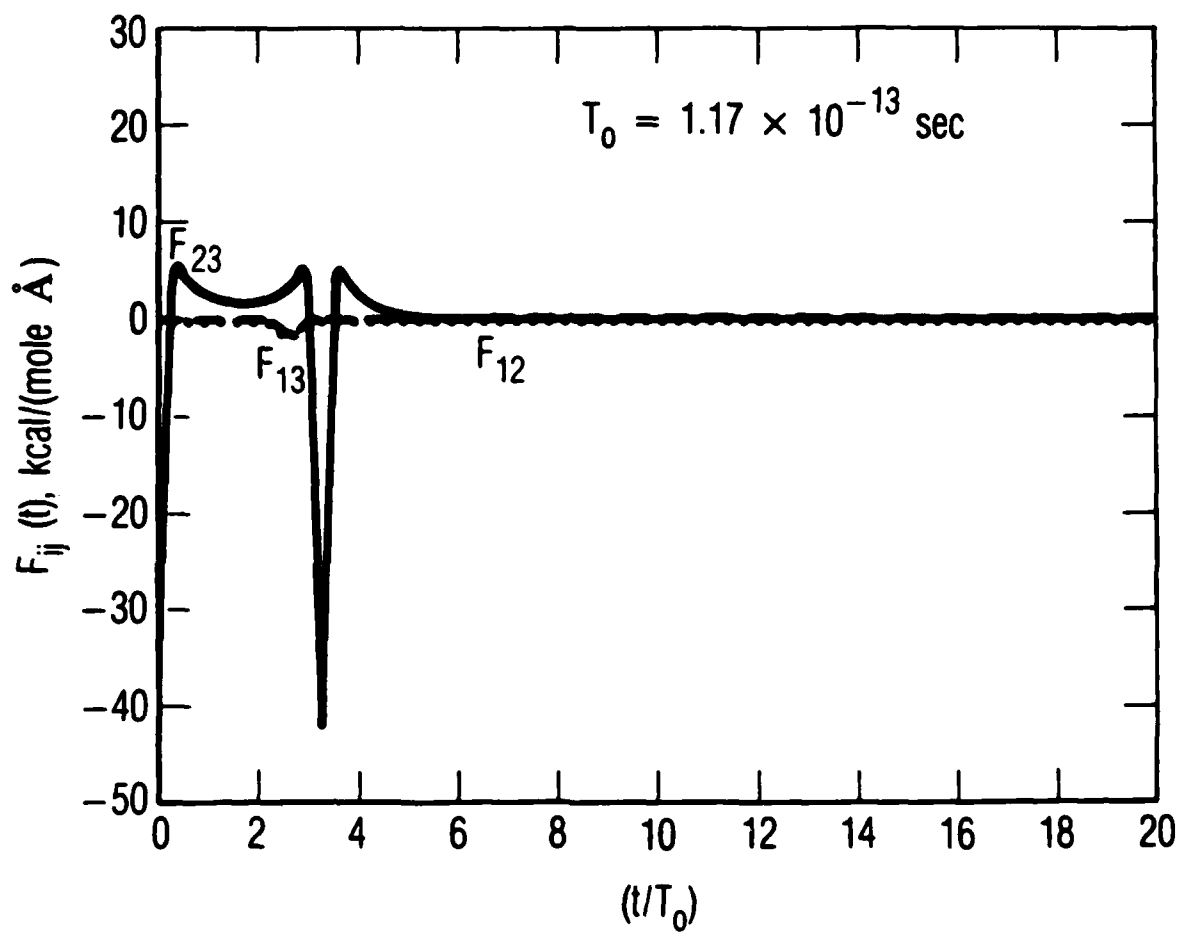


Fig. 5. Force Plot of Collision-Induced Dissociation of $\text{He} + \text{XeF}(v = 6, J = 10) \rightarrow \text{He} + \text{Xe} + \text{F}$. The force components F_{12} and F_{13} are quite small and correspond to the dashed and dotted curves, respectively.

The other type of collision that is observed on this surface that could lead to dissociation is shown in Fig. 6. This trajectory corresponds to a nonreactive inelastic collision. The initial relative translation energy of the reactants is converted into rotational energy of the product XeF molecule. The conversion of initial relative translational energy into product rotational energy (T-R) is the major energy transfer process, and the conversion of vibrational energy into rotational energy (V-R) is the minor energy transfer process. The additional rotational energy in the XeF molecule in this example is not sufficient to break the XeF bond, but in some trajectories where the additional rotational energy is sufficient to break the bond, we find it is prevented from doing so classically by the centrifugal barrier. This example is somewhat similar to that discussed by Clarke and Burns¹⁸ where in dissociation, molecules may climb a "rotational ladder" and then undergo intramolecular R-V energy transfer prior to the dissociative collision. The R-V energy transfer was not observed in our study, but we did observe V-R energy transfer. The dissociative collisions of XeF molecules with low vibrational energy are dominated by events in which the initial rotational energy makes the total internal energy close to the dissociation limit. Blais and Truhlar¹⁹ refer to states with internal energy above the dissociation limit which are prevented from dissociating classically by the centrifugal barrier as quasibound states. In our analysis, the unbound states include both quasibound states and completely dissociated states. We include the quasibound states in our analysis as dissociated states because, through calculations, we can show that such a vibrationally excited XeF molecule in a very high rotational state, upon collision with another He atom, will acquire sufficient relative translational energy necessary to dissociate the XeF molecule. Thus, multiple collisions provide another mechanism for dissociation of diatomic molecules.

Trajectory calculations were carried out on the He-XeF energy surface to follow the dynamics of vibrational excitation of XeF($v = 0$) by He atoms. A typical inelastic collision between He and XeF($v = 0$) is shown in Fig. 7. The process involved in this excitation is one in which a small fraction of the initial relative translational energy of the He-XeF system is converted into product vibrational energy of the XeF($v = 0$) molecule. Figure 7 shows that

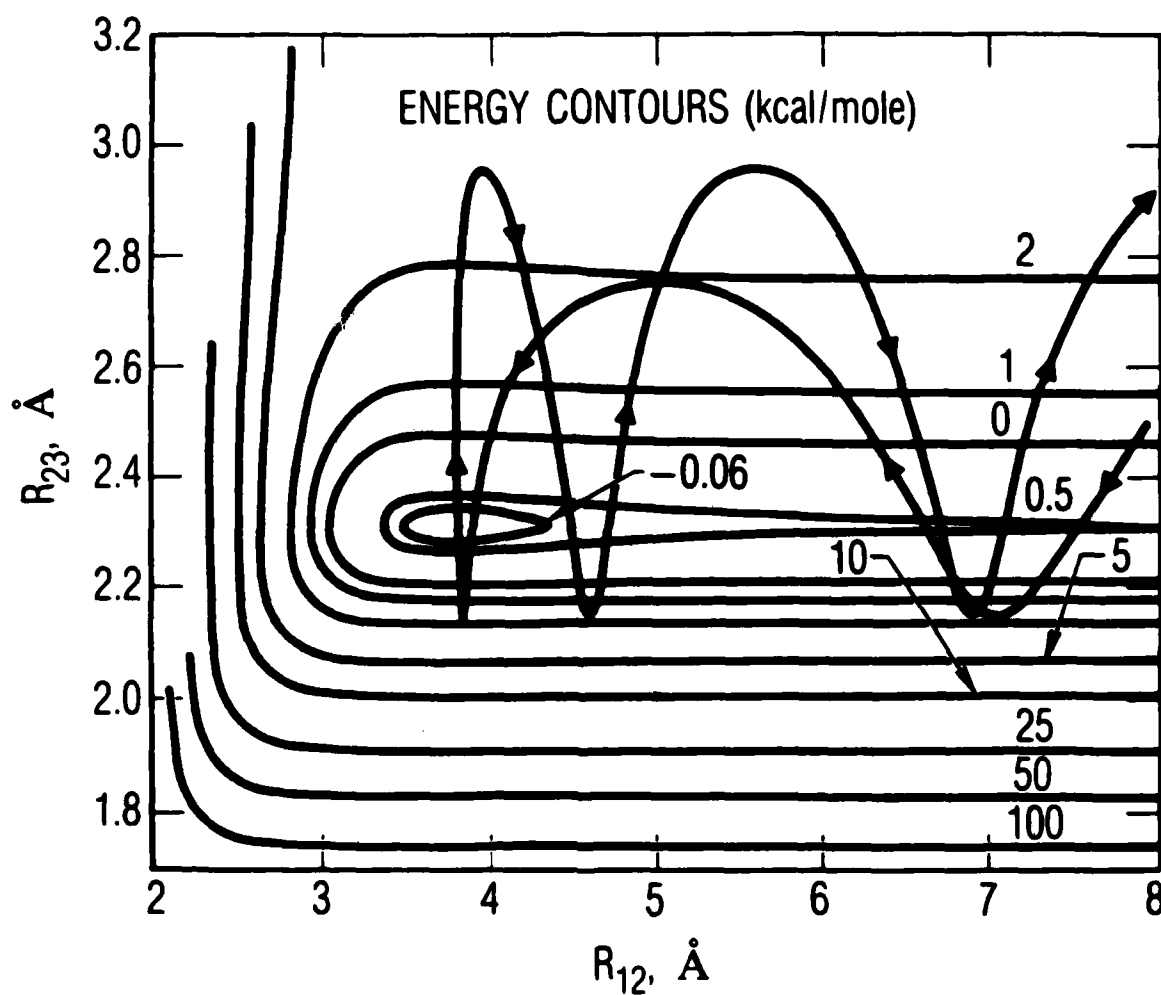


Fig. 6. Typical Inelastic Collision of $\text{He} + \text{XeF}(v = 3, J = 30) \rightarrow \text{He} + \text{XeF}(v' = 3, J = 50)$. The initial $E_{\text{TRANS}} = 1.5$ kcal/mole. For this system, T-R energy transfer is the major process, and V-R transfer is the minor energy transfer process.

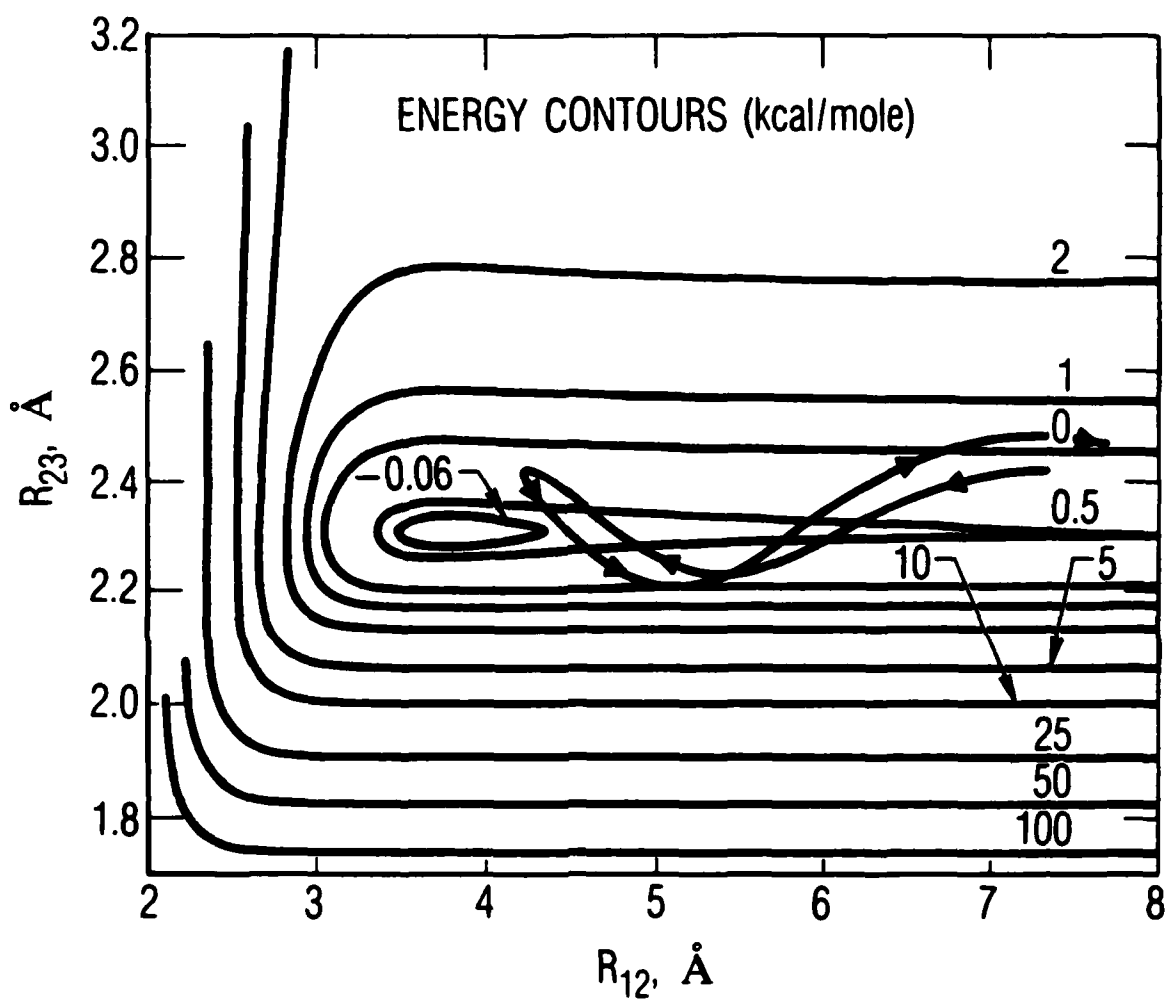


Fig. 7. Typical Inelastic Collision of $\text{He} + \text{XeF}(v = 0, J = 10) \rightarrow \text{He} + \text{XeF}(v' = 1, J = 13)$. A small fraction of initial relative translational energy (initial $E_{\text{TRANS}} = 5.5$ kcal/mole) is converted into product vibrational energy. Sufficient initial translational energy is converted into vibrational energy to change the vibrational state of XeF by one vibrational quantum.

oscillatory trajectory moves toward smaller R_{12} values, and thus the He atom is pulled closer to Xe. Finally, the representative mass point reaches a point on the surface where sufficient translational energy has been converted into vibrational energy of XeF to change the vibrational state of the initial XeF by one vibrational quantum; thus the He atom recedes from the XeF($v = 1$) molecule as the oscillatory trajectory moves toward larger R_{12} values. A very small fraction of the relative translational energy of the reactants goes into rotational energy of the product XeF molecule.

B. STATE-SPECIFIC RATE COEFFICIENTS

State-to-state rate coefficients have been calculated for collision-induced V-T and R-T rotational relaxation, and for dissociation processes from specific vibrational levels for collisions of XeF($v = 0$ through 8) with He atoms. Both temperature and v -dependences for the state-to-state rate coefficients were calculated for the relaxation processes. In addition, rotational relaxation rate coefficients have been calculated for collisions of He with ground state XeF(v, J).

The trajectory study predicts a mechanism favoring dissociation from states of high rotational quantum number at a specific vibrational quantum number. This trajectory study indicates that dissociation from low vibrational states is assisted by initial rotational excitation in the reactant molecule. This rotational bias has been observed in other quasiclassical calculations.^{20,21} The preference for vibrational energy in diatomic dissociation has been discussed by Kiefer et al.⁹ They show that the depletion of high vibrational states in the dissociation process is quite contrary to some theories, which assume the dissociation to take place from high vibrational states that are only slightly depleted in the process. In most of these theories,^{22,23} it is assumed that vibrational energy makes by far the dominant contribution to the energy required to dissociate the molecule.

State-to-state rate coefficients at room temperature computed by this study of collision-induced V-T and dissociation of XeF by He from several v -levels are shown by the solid lines in Fig. 8. The dashed lines show the results of a multilevel model developed by Fulghum et al.⁶ using surprisal

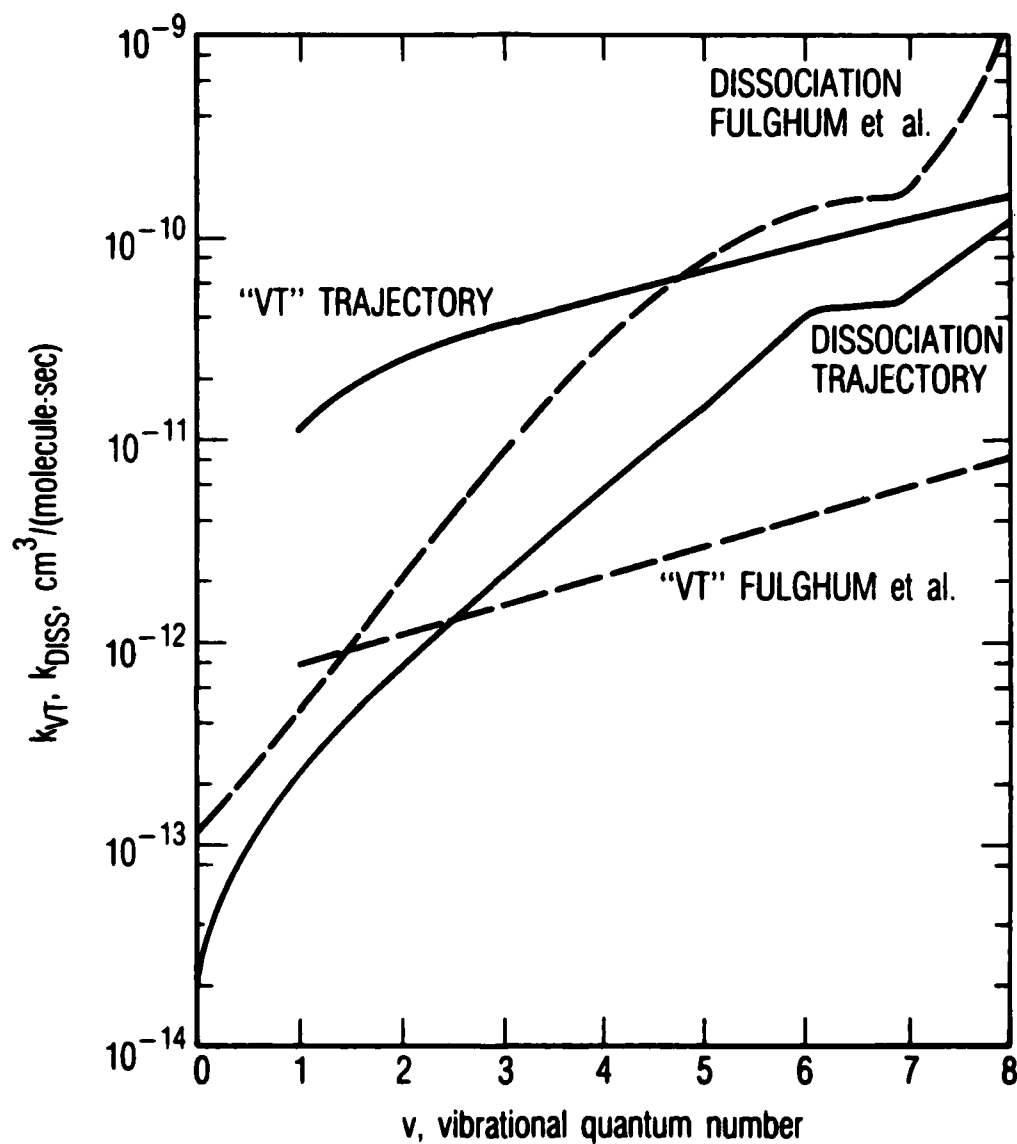


Fig. 8. State-to-State Rate Coefficients for Collisions of XeF with He, $T = 300$ K. Solid curves are results of the trajectory analysis. Dashed curves are the multilevel results of Fulghum et al.⁶

analysis to calculate V-T state-to-state rate coefficients and a variation of the Arrhenius equation to model the dissociation rates. Their experiments measured the total removal rates of the $v'' = 0$ and $v'' = 1$ vibrational levels of the ground electronic state of XeF. They attempted to extract from their measurements, values for the state-to-state V-T rates and direct dissociation rates out of the individual v-levels of XeF. The theoretical approach taken by Fulghum et al.⁶ was to fit the experimental data with a multilevel model that represents all of these state-to-state rates with only a few parameters. From Fig. 8, the Fulghum state-to-state V-T rate coefficients are a factor of 25 to 30 times smaller than those predicted from this trajectory study. However, the slopes for the two studies are almost identical from $v = 3$ to $v = 8$. The trajectory study indicates smaller values (the factors are 2 at $v = 1$, 4 at $v = 3$, and 10 at $v = 8$) for the dissociation rate coefficients than by the Fulghum et al.⁶ multilevel model. The state-to-state rate coefficients from the trajectory study, when used in a kinetic model, should predict a more efficient laser system than the Fulghum et al.⁶ model results for the following reasons: (1) The trajectory study predicts efficient V-T relaxation to populate the upper v-levels of ground state XeF where the XeF molecules are able to dissociate more easily, and (2) the Fulghum et al.¹⁻³ model is predicting very inefficient V-T relaxation and efficient dissociation even from the low v-states of XeF. It is difficult to understand from their model how the dissociation rate could be so effective even from the low v-states. The trajectory calculations show that the rate of dissociation from a specific vibrational level increases by a factor of 2 to 3 for an increase in temperature from 300 to 400 K. The observed increase in efficiency of the XeF laser in operating at 400 K instead of 300 K is about a factor of 2.²⁴

The trajectory study predicts that multiquanta vibrational transitions occur in the V-T vibrational relaxation processes. In Fig. 9 are shown the temperature dependences of the state-to-state rate coefficients for V-T vibrational relaxation processes exhibiting single-quantum vibrational transitions. The required temperature dependent rate coefficients for multiquanta V-T relaxation and collision-induced dissociation from a specific v-level are listed in Tables 2 and 3, respectively. The empirical form chosen is one commonly used in modeling nonequilibrium effects. These data will be

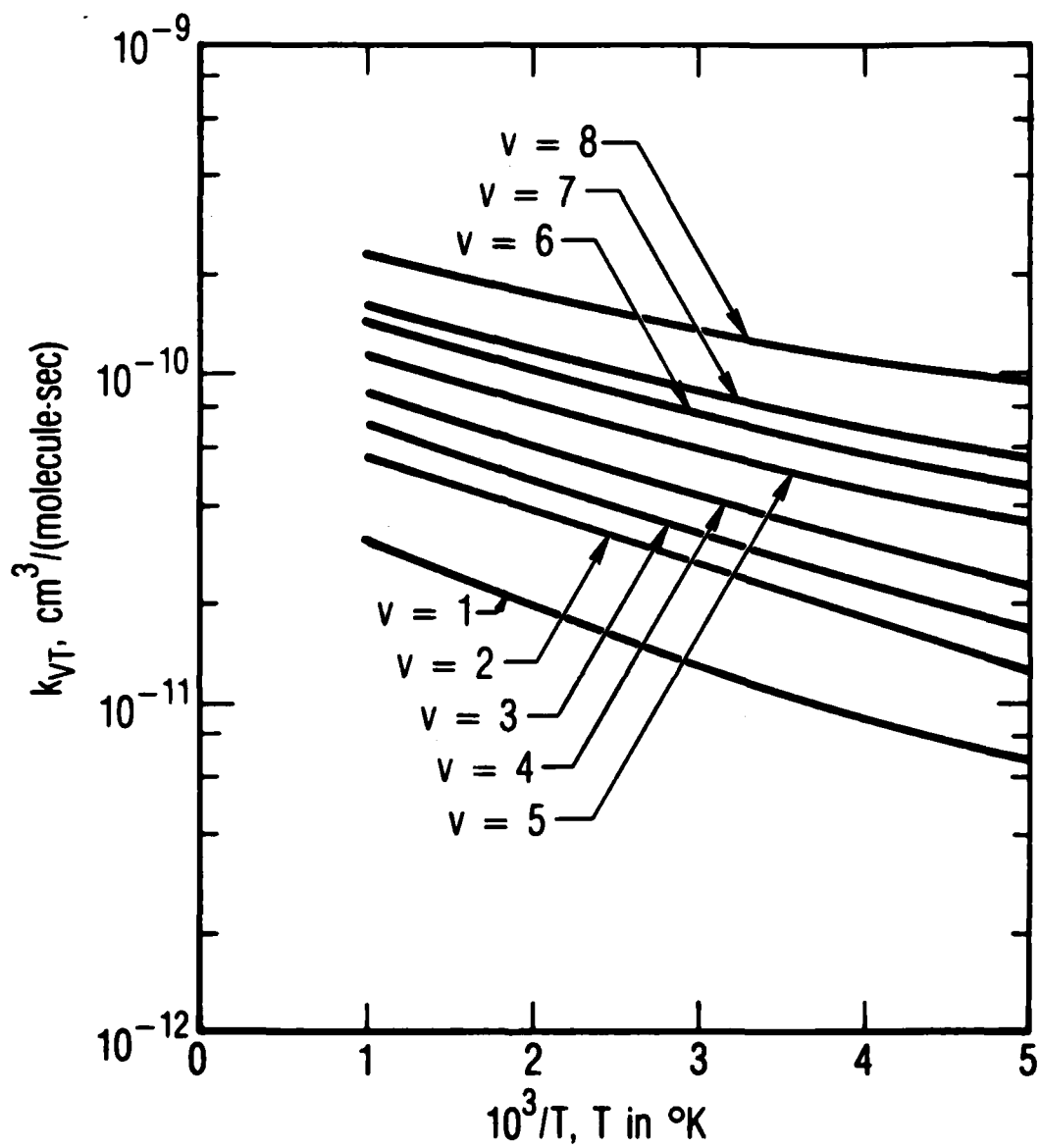


Fig. 9. Temperature Dependent V-T Rate Coefficients for Single Quantum Transitions for He + XeF (v) Collisions

Table 2. State-to-State Rate Coefficients for VT Relaxation of He + XeF (v)
from a Specific v-Level

$$k_{v,v'}(T) = A_{v,v'} T^n e^{-E/RT}, \text{ cm}^3/(\text{molecule-sec})$$

v	v'	$-\log_{10}(A_{v,v'})$	n	E cal/mole
0	1	9.1792	-0.458	1478.8
1	0	11.6463	0.415	432.2
2	1	10.2295	0.039	697.5
2	0	12.2211	0.466	981.3
3	2	9.6716	-0.106	803.6
3	1	11.8877	0.474	851.8
3	0	12.1096	0.377	883.2
4	3	10.0266	0.033	643.7
4	2	11.7468	0.404	545.9
4	1	11.2044	0.203	1296.1
5	4	9.7566	-0.018	598.4
5	3	10.5980	0.066	688.4
5	2	12.7361	0.663	478.8
6	5	9.4521	-0.087	631.0
6	4	10.7233	0.188	543.8
6	3	10.5122	-0.015	807.6
7	6	9.5660	-0.044	549.3
7	5	9.6753	-0.163	865.4
7	4	10.9432	0.099	433.6
8	7	9.3179	-0.061	535.9
8	6	10.3305	0.073	600.2
8	5	9.8242	-0.152	985.8

Table 3. Rate Coefficients for Dissociation of XeF (v) in Collision with He from a Specific v-Level

$$k_{\text{DISS}}(v', T) = A_v T^n e^{-E/RT}, \text{ cm}^3/(\text{molecule}\cdot\text{sec})$$

v	$-\log_{10}(A_v)$	n	E cal/mole
0	9.4622	-0.246	5049.9
1	8.0771	-0.792	3797.1
2	9.8420	-0.146	2714.0
3	9.2050	-0.270	2674.2
4	10.8763	0.270	1479.7
5	10.6871	0.250	986.0
6	10.2002	0.174	847.9
7	9.8615	0.097	940.3
8	9.6771	0.085	675.4

useful in modeling the performance of XeF excimer lasers. The V-T rate coefficients increase with increasing temperature and increasing v . The V-T rate coefficients do not have a v^n dependence, which is observed in relaxation of HF by several diluents.²⁵ The probability of V-T relaxation increases with increasing temperature and v -level. The trajectory study predicts that collision-induced V-T relaxation is extremely efficient in redistributing population into the higher vibrational states of ground state XeF.

The temperature dependences for the dissociation rate coefficients from $v = 0$ to $v = 8$ calculated from the trajectory study are shown in Fig. 10. Dissociation from $v = 0$ is a very ineffective process at low temperatures and becomes much more probable with increasing temperature. These data show that the probability of dissociation increases with increasing temperature and v -level. Thus at initial high vibrational levels, the conversion of reactant relative translational energy into product vibrational energy is more effective than the conversion of reactant relative translational energy into product rotational energy in promoting collision-induced dissociation. On the other hand, our trajectory study predicts that at initial low vibrational and high rotational levels, the conversion of reactant relative translational energy into product rotational energy is substantially more effective than the conversion of reactant relative translational energy into product vibrational energy in promoting collision-induced dissociation. This conclusion that initial vibrational energy is substantially more effective than rotational energy in promoting collision-induced dissociation is supported by a trajectory study by Dove and Raynor²⁶ on collisional dissociation of H_2 by He. Our trajectory data predict that, in collisions of He atoms with XeF molecules, translational energy is much more effective than rotation in promoting dissociation. Dove and Raynor²⁶ predicted that, in H_2 collisions with He, translational energy is less effective than rotational energy in promoting dissociation.

The v and temperature dependences of the rotational relaxation of XeF in collision with He are given in Figs. 11 and 12. The rotational relaxation rates are seen to have a slight v dependence and occur by multiquanta transitions. The dependence of the rotational relaxation rates at a specific

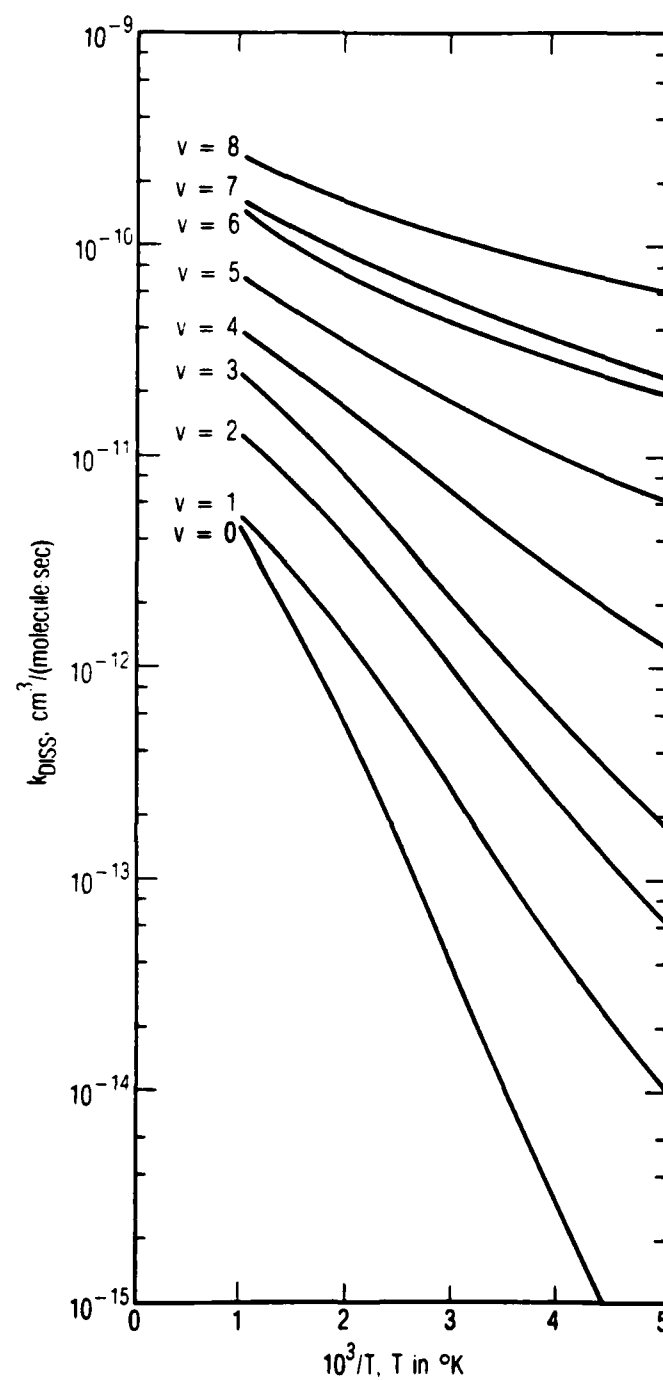


Fig. 10. Temperature Dependent Rate Coefficients for Dissociation from a Specific v -Level in $\text{He} + \text{XeF}(v)$ Collisions

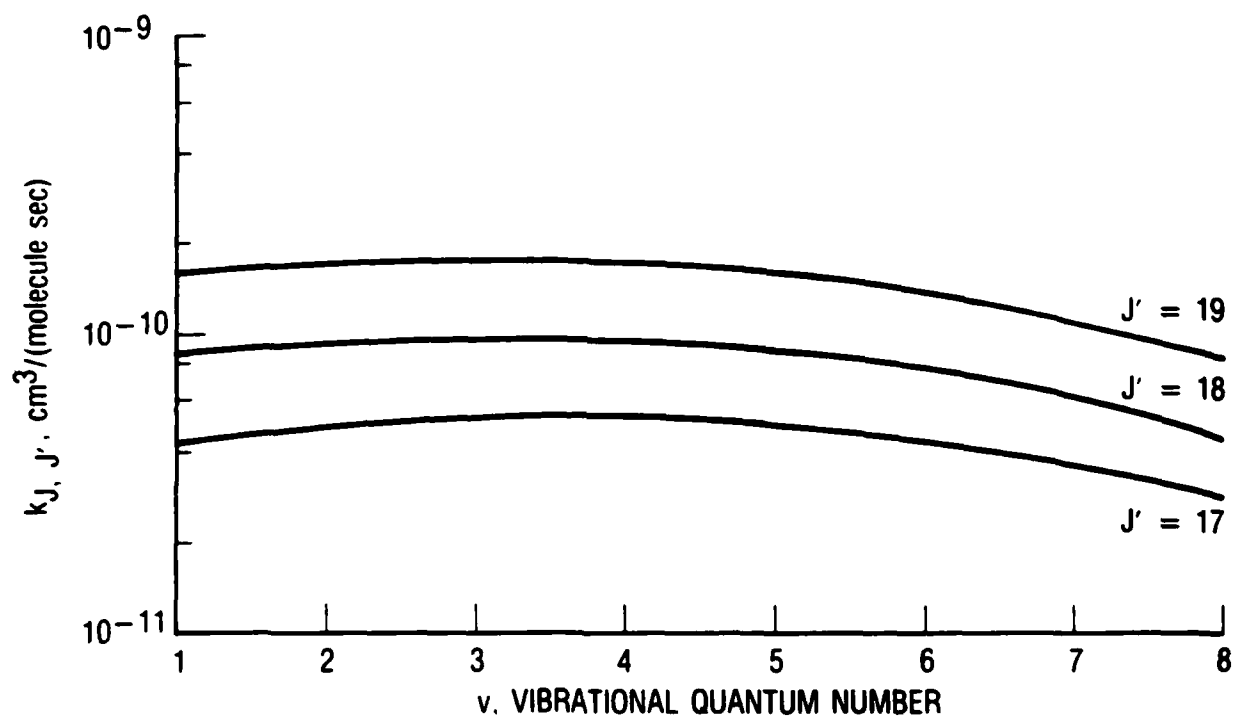


Fig. 11. The v -Dependence of Rotational Relaxation of $\text{XeF}(v, J = 20)$ in Collision with He

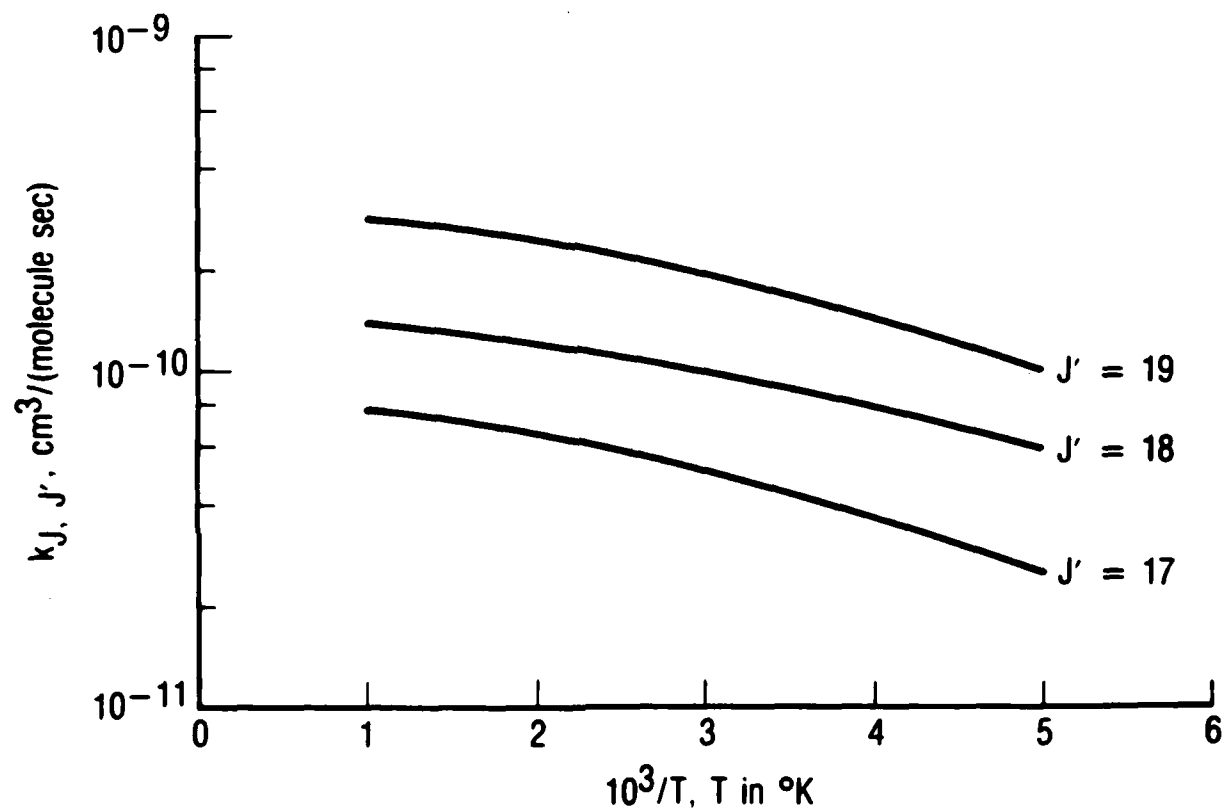


Fig. 12. Temperature Dependence of Rotational Relaxation for Collisions of $\text{XeF}(v = 3, J = 20)$ with He

v shows an increase with increasing temperature. Although there is not much dependence of the R-T rate on the vibrational quantum number or temperature, there is a large dependence on product rotational quantum number.

IV. SUMMARY

Quasiclassical trajectory analysis has been used to calculate both energy transfer and collision-induced dissociation rates from specific vibrational levels of XeF in collision with He. The resulting state-to-state rate coefficients provided by this study can be used to study model simulations of output efficiency and multilevel laser oscillations in XeF. The state-to-state specific rate coefficients have been compared with results obtained from the multilevel empirical models developed by Fulghum et al.⁶ The trajectory study predicted a mechanism favoring dissociation from states of low vibrational but high rotational states. The trajectory study predicts efficient V-T relaxation to populate the upper v-levels of ground state XeF, where XeF molecules are able to dissociate more easily. The temperature dependence of the rate coefficients indicates that the efficiency of an XeF excimer laser should improve by operating at higher temperatures, which is a result in agreement with experimental measurements.

REFERENCES

1. J. Tellinghuisen, P. C. Tellinghuisen, G. C. Tisone, J. M. Hoffman, and A. K. Hays, J. Chem. Phys. **68**, 5177 (1978).
2. P. C. Tellinghuisen, J. Tellinghuisen, J. A. Coxon, J. E. Velazco, and D. W. Setser, J. Chem. Phys. **68**, 5187 (1978).
3. P. C. Tellinghuisen and J. Tellinghuisen, Appl. Phys. Lett. **43**, 898 (1983).
4. S. F. Fulghum, I. P. Herman, M. S. Feld, and A. Javan, Appl. Phys. Lett. **33**, 926 (1978).
5. S. F. Fulghum, M. S. Feld, and A. Javan, Appl. Phys. Lett. **35**, 247 (1979).
6. S. F. Fulghum, M. S. Feld, and A. Javan, IEEE JQE, **16**, 815 (1980).
7. M. C. Gower, R. Exberger, P. D. Rowley, and K. W. Billman, Appl. Phys. Lett. **33**, 65 (1978).
8. I. Procaccia and R. D. Levine, J. Chem. Phys. **63**, 4261 (1975).
9. J. H. Kiefer, H. P. G. Joosten, W. D. Breshears, Chem. Phys. Lett. **30**, 424 (1975).
10. D. L. Huestis, Stanford Research Institute Report, No. MP-78-07, 113 (1978).
11. C. Duzy and V. H. Shui, paper DA-1, 31st. Annual Gaseous Electronic Conference, Buffalo, N.Y. 1978.
12. R. L. Wilkins, J. Chem. Phys. **63**, 534 (1975).
13. N. C. Blais and D. G. Truhlar, J. Chem. Phys. **65**, 5335 (1976).
14. D. L. Thompson, J. Chem. Phys. **78**, 1763 (1983).
15. R. A. Svehla, NASA Technical Report R-132 (1962).
16. B. Schneider, J. Chem. Phys. **58**, 4447 (1973).
17. R. G. Gordon and Y. S. Kim, J. Chem. Phys. **56**, 3122 (1972).
18. A. G. Clarke and G. Burns, J. Chem. Phys. **58**, 1908 (1973).
19. N. C. Blais and D. G. Truhlar, J. Chem. Phys. **78**, 2388 (1983); J. Chem. Phys. **70**, 2962 (1979).

20. N. J. Brown and R. J. Munn, J. Chem. Phys. 56, 1983 (1972).
21. A. Jones and J. L. J. Rosenfeld, Proc. Roy. Soc. A333, 419 (1973).
22. G. W. Tregay, W. G. Valance, and D. I. Mac Lean, J. Chem. Phys. 59, 1634 (1973).
23. H. Johnston and J. Birks, Accounts Chem. Res. 5, 327 (1972).
24. H. C. Hsia, J. A. Mangano, J. H. Jacob, and M. Rokni, Applied Phys. Lett. 34, 208 (1978).
25. N. Cohen, M. A. Kwok, R. L. Wilkins, and J. F. Bott, AIAA-83-1699, AIAA 16th Fluid and Plasma Dynamics Conference, July 12-14, 1983, Danvers, Mass.
26. J. E. Dove and S. Raynor, J. Chem. Phys. 28, 113 (1978).

LABORATORY OPERATIONS

The Aerospace Corporation functions as an "architect-engineer" for national security projects, specializing in advanced military space systems. Providing research support, the corporation's Laboratory Operations conducts experimental and theoretical investigations that focus on the application of scientific and technical advances to such systems. Vital to the success of these investigations is the technical staff's wide-ranging expertise and its ability to stay current with new developments. This expertise is enhanced by a research program aimed at dealing with the many problems associated with rapidly evolving space systems. Contributing their capabilities to the research effort are these individual laboratories:

Aerophysics Laboratory: Launch vehicle and reentry fluid mechanics, heat transfer and flight dynamics; chemical and electric propulsion, propellant chemistry, chemical dynamics, environmental chemistry, trace detection; spacecraft structural mechanics, contamination, thermal and structural control; high temperature thermomechanics, gas kinetics and radiation; cw and pulsed chemical and excimer laser development including chemical kinetics, spectroscopy, optical resonators, beam control, atmospheric propagation, laser effects and countermeasures.

Chemistry and Physics Laboratory: Atmospheric chemical reactions, atmospheric optics, light scattering, state-specific chemical reactions and radiative signatures of missile plumes, sensor out-of-field-of-view rejection, applied laser spectroscopy, laser chemistry, laser optoelectronics, solar cell physics, battery electrochemistry, space vacuum and radiation effects on materials, lubrication and surface phenomena, thermionic emission, photo-sensitive materials and detectors, atomic frequency standards, and environmental chemistry.

Computer Science Laboratory: Program verification, program translation, performance-sensitive system design, distributed architectures for spaceborne computers, fault-tolerant computer systems, artificial intelligence, micro-electronics applications, communication protocols, and computer security.

Electronics Research Laboratory: Microelectronics, solid-state device physics, compound semiconductors, radiation hardening; electro-optics, quantum electronics, solid-state lasers, optical propagation and communications; microwave semiconductor devices, microwave/millimeter wave measurements, diagnostics and radiometry, microwave/millimeter wave thermionic devices; atomic time and frequency standards; antennas, rf systems, electromagnetic propagation phenomena, space communication systems.

Materials Sciences Laboratory: Development of new materials: metals, alloys, ceramics, polymers and their composites, and new forms of carbon; non-destructive evaluation, component failure analysis and reliability; fracture mechanics and stress corrosion; analysis and evaluation of materials at cryogenic and elevated temperatures as well as in space and enemy-induced environments.

Space Sciences Laboratory: Magnetospheric, auroral and cosmic ray physics, wave-particle interactions, magnetospheric plasma waves; atmospheric and ionospheric physics, density and composition of the upper atmosphere, remote sensing using atmospheric radiation; solar physics, infrared astronomy, infrared signature analysis; effects of solar activity, magnetic storms and nuclear explosions on the earth's atmosphere, ionosphere and magnetosphere; effects of electromagnetic and particulate radiations on space systems; space instrumentation.

END

DATE

FILMED

5-88

DTIC